Protecting Polymers in Space with Atomic Layer Deposition Coatings

Timothy K. Minton,*,† Bohan Wu,† Jianming Zhang,† Ned F. Lindholm,† Aziz I. Abdulagatov,‡ Jennifer O'Patchen,‡ Steven M. George,‡ and Markus D. Groner§

Department of Chemistry and Biochemistry, Montana State University, Bozeman, Montana 59717, Department of Chemistry and Biochemistry, University of Colorado, Boulder, Colorado 80309, and ALD NanoSolutions, 580 Burbank Street, Unit 100, Broomfield, Colorado 80020

ABSTRACT Polymers in space may be subjected to a barrage of incident atoms, photons, and/or ions. Atomic layer deposition (ALD) techniques can produce films that mitigate many of the current challenges for space polymers. We have studied the efficacy of various ALD coatings to protect Kapton polyimide, FEP Teflon, and poly(methyl methacrylate) films from atomic-oxygen and vacuum ultraviolet (VUV) attack. Atomic-oxygen and VUV studies were conducted with the use of a laser-detonation source for hyperthermal O atoms and a D_2 lamp as a source of VUV light. These studies used a quartz crystal microbalance (QCM) to monitor mass loss in situ, as well as surface profilometry and scanning electron microscopy to study the surface recession and morphology changes ex situ. Al_2O_3 ALD coatings protected the underlying substrates from atomic-oxygen attack, and the addition of TiO_2 coatings protected the substrates from VUV-induced damage. The results indicate that ALD coatings can simultaneously protect polymers from oxygen-atom erosion and VUV radiation damage.

KEYWORDS: polymer protection • low Earth orbit • atomic layer deposition • atomic oxygen erosion • VUV photodegradation

INTRODUCTION

Spacecraft in low Earth orbit (LEO) are subject to a number of damaging phenomena including atomic oxygen, electromagnetic radiation, ions, and electrons (1, 2). LEO altitude environments, which range from 200 to 700 km, contain predominantly atomic oxygen and molecular nitrogen, which collide with spacecraft surfaces at relative velocities of ~7.4 km s^{-1} (3). These high velocities lead to high energy gas-surface collisions equivalent to O atoms with ~450 kJ mol^{-1} of translational energy colliding with the surface (4). Structural and thermal-control materials consisting of organic polymers are particularly susceptible to oxygen-atom attack. High-energy collisions lead to the production of volatile products that carry mass away from the polymer surface and leave a roughened surface that scatters light (5). Polymeric materials on spacecraft in LEO are also susceptible to high fluxes of vacuum ultraviolet (VUV) radiation, which may promote their degradation through multiple photochemical processes. Photons might act either alone or in combination with oxygen atoms to degrade polymers and paints and thus limit their usefulness (6). Given the harsh environment in LEO, steps must be taken to protect polymers that are to be used on spacecraft that operate in this environment.

The most common method employed for protection of polymeric materials from the harsh environment of LEO has been the application of a protective inorganic coating, such as SiO_2, which is relatively unreactive to atomic oxygen (7). These protective coatings are usually deposited by plasma enhanced chemical vapor deposition (PECVD). PECVD methods are limited to line-of-sight targets. In addition, films produced by PECVD are found to have large defect densities because of their columnar nature, thus leaving the underlying polymer vulnerable to atomic-oxygen attack. Therefore, relatively thick coatings must be used to reduce the defect density. SiO_2-coated Kapton polyimide surfaces with a thickness of 1300 Å have demonstrated erosion yields as low as ~0.1−0.2% of unprotected Kapton (8).

Alternative solutions to inorganic coatings have been explored through the development of inorganic/organic copolymers that utilize the reaction of atomic oxygen with the inorganic component to form a protective oxide layer. Possible replacement of Kapton by copolymers containing polyoligomeric silsequioxane has been suggested (9). However, these polymers still exhibit finite levels of erosion by atomic oxygen and their stability with respect to VUV radiation has not been studied. Another proposed solution is to imbed Si containing groups into the polymer up to 1 μm via the Photosil process. The modified surface is converted to a silica layer when exposed to an oxidizing environment (10). This process has shown promise, especially for flat substrates, but this process is still mainly a line-of-sight method.

The work described here investigates a new approach to protect polymers from both atomic oxygen and VUV light that might have a damaging effect in LEO. This approach is

* To whom correspondence should be addressed. Tel: 406-994-5394. Fax: 406-994-6011. E-mail: tminton@montana.edu.
Received for review March 13, 2010 and accepted August 5, 2010
† Montana State University.
‡ University of Colorado.
§ ALD NanoSolutions.
DOI: 10.1021/am100217m

based on atomic layer deposition (ALD), which is a variation of chemical vapor deposition (CVD) that does not rely on line-of-sight and does not employ the high substrate temperatures that CVD typically requires. ALD is a gas-phase method based on two sequential, self-limiting surface reactions, producing continuous, Angstrom-level-controlled, defect-free films (11). Al_2O_3 ALD is a particularly well-defined system (12, 13) that has been successfully deposited on polymer substrates (14, 15). Al_2O_3 ALD coatings are pinhole-free, as demonstrated by electrical measurements (16). The Al_2O_3 ALD coatings have been observed to have excellent gas diffusion barrier properties on both polyethylene naphthalate (PEN) and Kapton polymer substrates (17, 18). An earlier study utilizing Al_2O_3 ALD coatings for protection of polyimide substrates against hyperthermal oxygen atoms conducted in our laboratory determined that coating thicknesses of ~35 Å were successful at preventing erosion (19). ALD coatings can be tailored for VUV absorption, as well as atomic-oxygen protection.

Al_2O_3 ALD can be used to illustrate the basic principles of ALD. Al_2O_3 is a binary material. The binary reaction for Al_2O_3 is $2Al(CH_3)_3 + 3H_2O \rightarrow Al_2O_3 + 6CH_4$. This binary reaction can be divided into two reactions to define Al_2O_3 ALD (12, 13)

$$(A)AlOH^* + Al(CH_3)_3 \rightarrow AlOAl(CH_3)_2^* + CH_4 \quad (1)$$

$$(B)AlCH_3^* + H_2O \rightarrow AlOH^* + CH_4 \quad (2)$$

where the asterisks indicate the surface species. If each reaction is self-limiting and self-terminating, then the repetitive application of these reactions in an ABAB... sequence can produce atomic layer controlled Al_2O_3 deposition. Al_2O_3 ALD can be deposited at the low temperatures required for coating polymers (14, 15).

Other chemistries permit the deposition of a variety of different coatings, such as ZnO, TiO_2, and SiO_2, and multilayer coatings of different composition are possible. For the ALD of TiO_2 and SiO_2 films, the $MCl_4 + 2H_2O \rightarrow MO_2 + 4HCl$ reaction for MO_2 deposition (where M = Si or Ti) is divided into the following two half-reactions (20–22)

$$(A)MOH^* + MCl_4 \rightarrow MOMCl_3^* + HCl \quad (3)$$

$$(B)MCl^* + H_2O \rightarrow MOH^* + HCl \quad (4)$$

We have studied the efficacy of various ALD coatings to protect Kapton polyimide, FEP Teflon, and poly(methyl methacrylate) (PMMA) films from atomic-oxygen and VUV attack in simulated LEO environments. We have found that such coatings can be highly effective at blocking degradation of the polymer substrates by these potentially damaging environmental agents.

EXPERIMENTAL DETAILS

Sample exposures were conducted in the source region of a molecular beam apparatus (9, 23–25), pictured in Figure 1. A pulsed, hyperthermal, O-atom beam was produced with the use of a laser-detonation source. The source produces a beam of both neutral O atoms (75–90%) and molecular O_2 (10–25%) traveling at velocities of ~8 km s^{-1}. The average translational energy of the hyperthermal O atoms was in the 500 – 520 kJ mol^{-1} range.

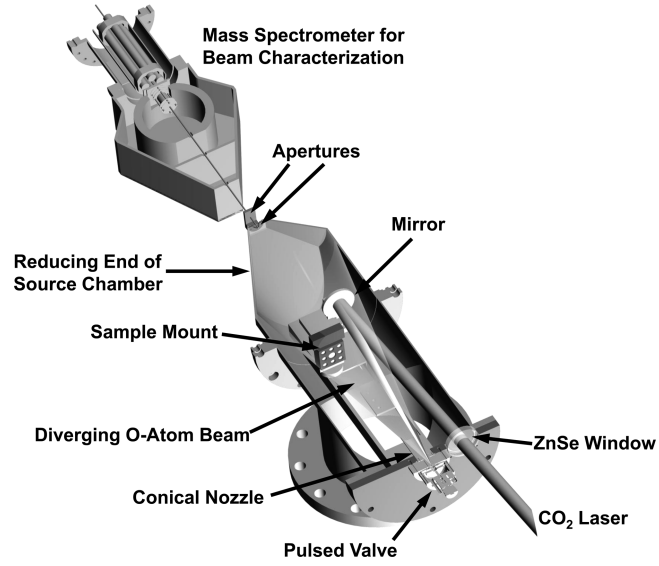

FIGURE 1. Schematic diagram of hyperthermal O-atom apparatus. A QCM head can be placed in the same position as the sample mount.

The coated and uncoated control samples were mounted in a custom, 9-position sample holder described previously (25). Stainless steel screens were placed over the samples to facilitate measurement of surface recession. The samples were exposed to the hyperthermal O-atom beam at a repetition rate of 2 Hz, for 100 000 pulses. Postexposure step-height measurements were conducted with the use of a Dektak-3 (Veeco Metrology Group) surface profiler. The average erosion depth and associated standard deviation for each sample were calculated from 40–50 different step heights. Uncoated Kapton H control samples were placed in the center position of the mount for each exposure, in order to quantify the fluence of O atoms. The LEO equivalent AO fluences were calculated from recession measurements by taking the erosion yield of Kapton H to be 3.00×10^{-24} cm^3 O-$atom^{-1}$ (25). The erosion yields of the test samples were calculated based on their recession relative to that of the relevant Kapton H control samples. Additional analysis of surface morphologies was conducted with field-emission scanning electron microscopy (FE-SEM).

Quartz crystal microbalance (QCM) sensors were used to study the efficacy of ALD films for VUV radiation protection. PMMA substrates were prepared using a solution of 20 wt % of polymer (Scientific Polymer Products Inc. #424 MW = 15,000) in chlorobenzene. The solution was then spin-coated at 2000 rpm for 1 min onto 0.5 in. diameter QCM discs. After spin coating, the samples were allowed to dry in air and then placed in a vacuum furnace and cured at 120 °C for 10 h. The PMMA films on the QCM disks were ~2 μm thick. The PMMA substrates were then coated with varying thicknesses of Al_2O_3 ALD. In some cases, an additional ALD coating of TiO_2 was deposited.

Table 1 contains a list of the samples used for VUV exposure studies. One cycle refers to the application of one AB ALD coating sequence, according to reactions 1 and 2 for Al_2O_3 ALD or reactions 3 and 4 for TiO_2 ALD. The ALD films were grown at 90 °C in a hot-wall viscous flow reactor (26). The films were deposited using a pulse sequence of (t_1, t_2, t_3, t_4) = (1, 30, 1, 30) where t_1 is the pulse time for the $Al(CH_3)_3$ (or $TiCl_4$), t_2 is the N_2 purge time, t_3 is the pulse time for the H_2O, and t_4 is the pulse

Table 1. ALD Coatings on PMMA Samples used for VUV Exposures

sample no.	ALD coating	total thickness (Å)
1	20 cycles (Al_2O_3) + 25 cycles (TiO_2)	26
2	20 cycles (Al_2O_3) + 50 cycles (TiO_2)	47
3	20 cycles (Al_2O_3) + 100 cycles (TiO_2)	81
4	20 cycles (Al_2O_3) + 200 cycles (TiO_2)	147
5	30 cycles (Al_2O_3)	23
6	58 cycles (Al_2O_3)	58
7	73 cycles (Al_2O_3)	74
8	145 cycles (Al_2O_3)	152

time for the second N_2 purge time. All times are in seconds. Following the nucleation period, the Al_2O_3 ALD and TiO_2 ALD growth rates at 90 °C are 1.1 and 0.6 Å/cycle, respectively. The total film thicknesses were obtained from X-ray reflectivity (XRR) measurements performed on silicon wafers that were deposited at the same time as the PMMA samples. The XRR data were acquired by a high-resolution Bede D1 Diffractometer (Bede Scientific) using a Cu K_α X-ray tube with a wavelength of 1.54 Å. The film thicknesses were extracted using the REFS data fitting software from Bede Scientific.

VUV radiation was supplied by a 30 W deuterium lamp (Hamamatsu model L7292) at a distance of ~40 cm. At this distance, the intensity of radiation in the wavelength range 115−200 nm is ~8 solar equivalents (or "suns") in low Earth orbit. The mass loss as a result of the VUV exposure was measured in situ with the use of a Maxtek QCM head (Model DSH200) and Model RQCM data collection system. The VUV flux decreased during each exposure, and the relative flux was measured with a phototube (Hamamatsu R1187). The recorded VUV relative flux during each exposure was fitted to a function as shown in Figure 2. The measured mass loss as a function of time was normalized to the VUV flux by dividing the raw mass loss measurement by the relative VUV flux (determined by the fitting function) at a series of exposure times. Before each new exposure, the window of the D_2 lamp was cleaned, and after each cleaning, the relative flux returned approximately to its initial value from the previous exposure. Thus, we concluded that the main cause of the VUV flux reduction during an exposure was photoinduced contamination on the lamp window.

RESULTS AND DISCUSSION

Two sets of atomic oxygen exposures with Al_2O_3 ALD coatings of varying thicknesses were carried out on both

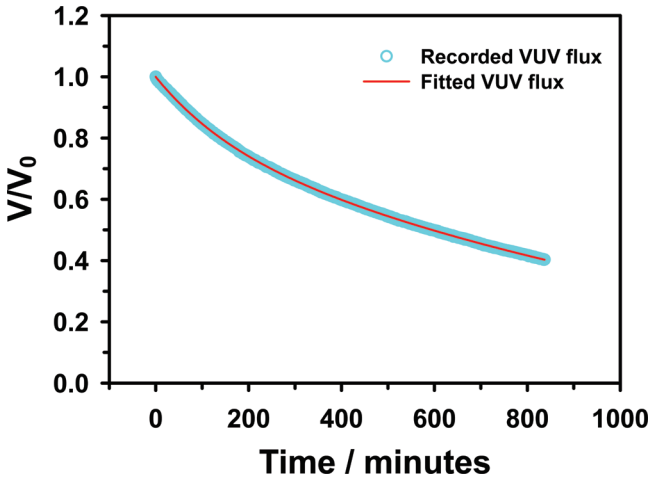

FIGURE 2. Relative VUV flux from D_2 lamp, measured with a photodiode, as a function of time at the position of the samples mounted on the QCM head.

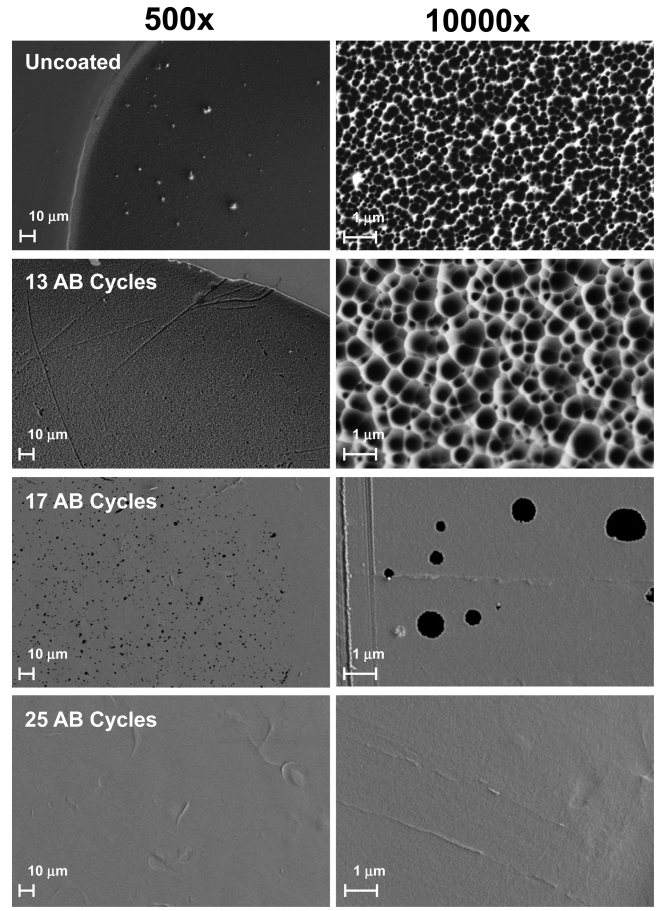

FIGURE 3. FE-SEM images of uncoated Kapton H and Kapton H coated with 13, 17, and 25 Al_2O_3 ALD AB cycles, after exposure to atomic oxygen. The left and right columns display images of the exposed areas of the samples collected with ×500 and ×10 000 magnification, respectively. The images in the left column show regions where the samples were exposed and where they were covered by part of a stainless steel screen. The images in the right column show only exposed regions of the samples. The 13-cycle sample displays a surface morphology similar to that of the uncoated sample, indicating that the coating did little to protect the polymer. The 17-cycle sample displayed an erosion pattern that was visible to the naked eye, but without a measurable profilometry reading. The visible pattern was revealed to be several small holes, as seen in the images. The 25-cycle sample displayed no erosion, indicating successful protection of the polymer substrate against O-atom attack.

Kapton H and FEP Teflon free-standing films. The first set included Kapton H coated with 13, 17, 25, 40, 50, and 100 AB cycles of Al_2O_3, as well as an uncoated Kapton H control sample. These Al_2O_3 ALD coatings were performed using a pulse sequence of (1, 120, 1, 120) at a temperature of 90 °C. Postexposure profilometry measurements recorded step heights only for the uncoated Kapton H control and the sample with 13 cycles of Al_2O_3 ALD. A faint erosion pattern was observed on the sample with 17 cycles of coating, but no step height could be measured via profilometry. None of the samples with 25 cycles of Al_2O_3 ALD or higher displayed any erosion.

FE-SEM images were recorded to probe the surface recession and morphology in greater detail. Figure 3 displays FE-SEM images, at low (500×) and high (10 000×) magnification, of exposed samples of uncoated Kapton H and

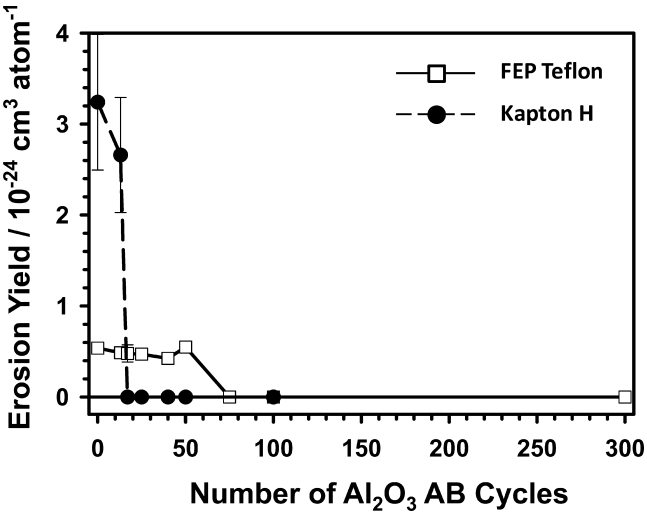

FIGURE 4. Plot of erosion yield of FEP Teflon and Kapton H samples as a function of number of Al_2O_3 ALD AB cycles. The FEP Teflon required many more cycles to protect against O-atom erosion, indicating a slower coating-nucleation process on FEP Teflon.

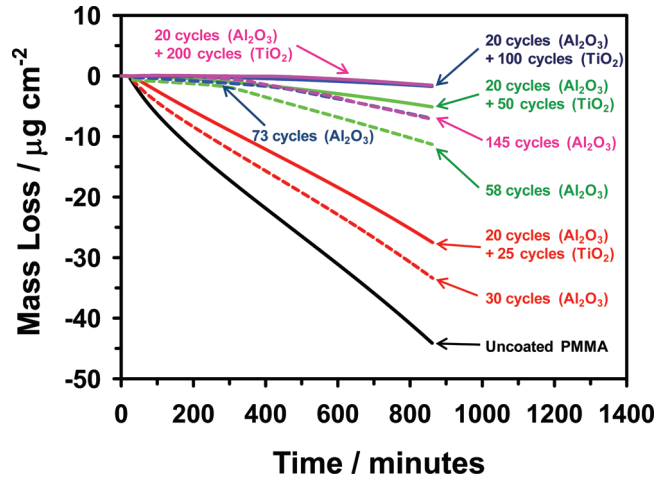

FIGURE 5. Mass change of PMMA substrates, coated with varying numbers of Al_2O_3 and TiO_2 ALD AB cycles, versus exposure time to VUV radiation from a D_2 lamp. The mass loss values presented are the result of normalizing the raw mass loss measurements to the relative flux of the D_2 lamp. The Al_2O_3 ALD coated samples displayed less mass loss than the bare (uncoated) PMMA sample, possibly because the coatings block the release of volatile products. The mass-loss curves of the TiO_2/Al_2O_3 coated samples indicate that a TiO_2 layer may protect the substrate from VUV-induced photodegradation.

samples coated with 13, 17, and 25 AB cycles of Al_2O_3. The faint erosion pattern observed on the 17-cycle sample was determined to be small round defects, similar in nature to the defects observed in the earlier study in our laboratory (19). Upon comparison with the earlier study, Al_2O_3 ALD appears to protect Kapton H with fewer AB cycles than that required to protect Kapton-like polyimide (Pyralin) films. This result suggests faster nucleation of the Al_2O_3 ALD coating on commercial Kapton H compared with the lab-prepared polyimide, despite their sharing the same chemical repeat unit.

A second series of Al_2O_3 ALD coatings were deposited on FEP Teflon, with the same numbers of AB cycles that were used in the Kapton study: 13, 17, 25, 40, 50, and 100 cycles. The FEP Teflon surface was not pretreated prior to ALD deposition. These Al_2O_3 ALD coatings were also deposited at 90 °C using a pulse sequence of (1, 120, 1, 120). Unlike the Kapton H samples, nearly all coated samples displayed erosion from atomic-oxygen exposure, with only the 100-cycle sample being free of measurable erosion. An additional group of Al_2O_3 ALD FEP Teflon samples (50, 75, 100, and 300 cycles) were exposed to the hyperthermal O-atom beam. Of this group, only the 50-cycle sample displayed any measurable erosion. This erosion was similar in depth to the 50-cycle sample from the first set of coated FEP Teflon samples. The samples coated with 75 and 100 cycles displayed an erosion pattern that was visible to the naked eye, but no step height was measurable by profilometry. The 300-cycle sample appeared to be unaffected by the O atoms, even when examined by FE-SEM.

Figure 4 displays a plot of erosion yield as a function of number of AB cycles for both Kapton H and FEP Teflon substrates. The threshold for sufficient O-atom protection is >15 cycles on Kapton H. In contrast, the threshold for sufficient O-atom protection is near 100 Al_2O_3 AB cycles on FEP Teflon. This difference is probably explained by the greater number of AB cycles required to nucleate the Al_2O_3 ALD coating on FEP Teflon. FEP Teflon is more inert and the $Al(CH_3)_3$ and H_2O are not expected to diffuse into FEP Teflon as easily as Kapton H. The initial diffusion of $Al(CH_3)_3$ and H_2O into the polymer is required for the nucleation of the Al_2O_3 ALD coating (14). This initial reactant diffusion is apparently much less on FEP Teflon than on Kapton H. Nevertheless, ALD is still able to form a passivating Al_2O_3 coating on FEP Teflon even with no surface pretreatment.

ALD-coated PMMA was used to study the efficacy of ALD coatings for VUV protection. PMMA was chosen as a substrate because of its known propensity to degrade under VUV radiation (27). PMMA films on QCM discs were coated with either Al_2O_3 ALD alone, or with a base layer of Al_2O_3 ALD followed by an additional coating of TiO_2 ALD. The Al_2O_3 ALD was needed prior to the TiO_2 ALD because TiO_2 ALD did not nucleate well on the PMMA surfaces without the Al_2O_3 ALD base layer. As shown in Table 1, there are eight samples with four nominal total coating thicknesses: ~25, ~50, ~75, and ~150 Å. The total thickness of sample 1 is less than the thickness expected from the nominal growth rates of Al_2O_3 ALD and TiO_2 ALD because of nucleation effects. An attempt was made to produce four pairs of samples, with each pair having approximately the same overall coating thickness. For each pair, one sample has a coating of pure Al_2O_3, and one sample has an Al_2O_3 adhesion layer followed by a TiO_2 coating. This study was designed to evaluate the effect of VUV light (from a D_2 lamp) on the PMMA substrate and separate the role of the overall coating acting as a gas barrier from the role of the TiO_2 ALD coating acting as a VUV filter.

Figure 5 contains the normalized mass-loss data collected by the QCM when PMMA films with various coatings were exposed to VUV light from the D_2 lamp. The uncoated PMMA shows significant mass loss with time, presumably because of the release of methyl formate as PMMA photodegrades

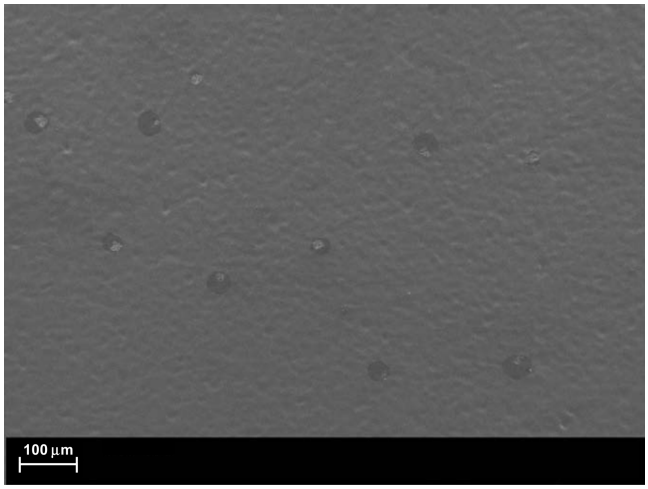

FIGURE 6. FE-SEM image of PMMA substrate coated with 145 cycles (Al_2O_3) with total thickness of 152 Å after 14 h exposure to a deuterium lamp with a flux of ~8 solar equivalents. Round areas ("blisters") where the coating has been removed are evident.

under VUV exposure (27−30). The Al_2O_3 ALD coated samples displayed a significant reduction in mass loss compared with the uncoated PMMA. Al_2O_3 does not absorb significantly in the VUV region of the spectrum and was therefore not expected to protect the substrate against VUV radiation. The reduction in mass loss on Al_2O_3-coated PMMA suggests that the Al_2O_3 coating may be acting as a physical barrier that blocks the release of gaseous products that are produced by photodegradation.

As gaseous photoproducts are released from the PMMA substrate, they would be expected to increase the pressure underneath the ALD coating. If the coating is very thin, then the products may escape slowly by diffusing through the coating, or products may be released if the coating becomes compromised as gaseous products form at the interface between the substrate and coating and cause delamination. Products that do not readily escape might rereact with the substrate. If the coating is thick enough to block diffusion, then the pressure may build to the point where the coating ruptures, in which case the gaseous products will be released and perhaps will also carry away a portion of the coating.

This mechanism is supported by the scanning electron micrograph of the sample with the thickest Al_2O_3 ALD coating shown in Figure 6. This figure indicates the formation of defects, or blisters, in the coating that allow more gaseous products to escape. The observation of specific points where the coating ruptured as opposed to general peeling of the coating suggests that delamination of the coating was not an important degradation mechanism. However, evidence of delamination would be more obvious with the thicker coatings. Delamination could possibly be occurring, in addition to diffusion through the coating, when a polymer with a thin coating is exposed to VUV light. Studies of coating adhesion before and after VUV exposure may lead to further understanding of the mechanisms of coating failure when a coated polymer is irradiated with VUV light.

For sample pairs of a given total coating thickness, the sample that had an additional coating of TiO_2 ALD exhibited substantially less mass loss than the samples coated only with Al_2O_3 ALD. The reduced mass loss of the TiO_2 ALD coated samples cannot be attributed to a barrier effect alone, because TiO_2 and Al_2O_3 ALD coatings had approximately the same total thickness. Thus, we conclude that the TiO_2 ALD coating reduced the flux of VUV light that reached the substrate and the consequent release of volatile products. For TiO_2 ALD coatings of 100 and 200 cycles (~60 and ~125 Å, respectively), the mass loss was negligible. This behavior indicates that these coatings provided essentially complete VUV protection, with respect to mass loss, at the tested flux and exposure duration.

Given the absorption coefficient of 1.0×10^6 cm^{-1} (31), and the assumption of a 125 Å thick coating, we estimate that ~30% of the incident VUV radiation would be absorbed by the 200-cycle TiO_2 coating. Therefore, a significant fraction of the incident VUV light should have penetrated the coating, possibly inducing photochemistry in the polymer substrate even when no mass loss was observed. If gaseous photoproducts are trapped by the coating and are able to rereact before leaving the polymer, then chemical changes could occur that are undetectable by mass loss measurements. Further spectroscopic studies of the substrate chemistry of coated polymers that are exposed to VUV light would thus be desirable.

Without knowing how the substrate chemistry changes or the rate of such changes, we cannot be sure what the performance of a polymer would be in LEO with the thickest TiO_2 coating tested. At the lower VUV fluxes of the LEO environment, the rate of photoproduct production would be much less than that of our exposure conditions. The coating might be able to contain the photoproducts indefinitely while the underlying polymer undergoes chemical transformation and degradation of function. Alternatively, the reduction in VUV light provided even by an optically thin coating in conjunction with the gaseous-barrier effect provided by the coating may slow the photodegradation process and allow the substrate to anneal the photoinduced defects (or "heal" itself) before products could escape. In this case, even the tested coatings might significantly enhance the useful lifetime of a polymer in LEO.

Blocking all VUV light from the substrate would be advantageous. Thicker coatings may be used, but these might be more prone to cracking. An approach to mitigate cracking and still produce optically thick coatings would be to deposit multilayer coatings of TiO_2 and a polymer, which we are currently investigating. Although further work remains to be done, the results presented here demonstrate the potential of VUV-absorbing ALD coatings to protect a polymer substrate from photochemical damage.

CONCLUSION

Atomic layer deposition of Al_2O_3 and TiO_2 on polymers produces coatings that can protect the substrate against both atomic-oxygen erosion and VUV-induced degradation in a space environment. While Al_2O_3 ALD coatings were found to protect both FEP Teflon and Kapton H, many more ALD cycles were required to protect FEP Teflon from O-atom

erosion. This behavior suggests a much more rapid nucleation of the ALD coating on Kapton H. Bilayer Al_2O_3 and TiO_2 ALD coatings were found to be effective in preventing mass loss in PMMA that was exposed to VUV radiation. The VUV studies revealed that if any light penetrates the coating, then the polymer substrate may release volatile products that can jeopardize the integrity of the coating.

Acknowledgment. This work was supported by a grant from the Air Force Office of Scientific Research (FA9550-07-C0139).

REFERENCES AND NOTES

(1) Edwards, D. L.; Tighe, A. P.; Van Eesbeek, M.; Kimoto, Y.; de Groh, K. *MRS Bull.* **2010**, *35*, 25.
(2) Grossman, E.; Gouzman, I. *Nucl. Instrum. Methods Phys. Res., Sect. B* **2003**, *208*, 48.
(3) Murad, E. *J. Spacecr. Rockets* **1996**, *33*, 131.
(4) Banks, B. A.; de Groh, K. K.; Rutledge, S. K.; DiFilippo, F. J. *NASA Technical Memorandum 107209*; National Aeronautics and Space Administration: Washington, D.C., 1996.
(5) Minton, T. K.; Garton, D. J. Dyanmics of Atomic-Oxygen Induced Polymer Degradation in Low Earth Orbit.\. In *Chemical Dynamics in Extreme Environments*; Dressler, R. A., Ed.; Advanced Series in Physical Chemistry; World Scientific: Singapore, 2001; Vol. 11; p 421.
(6) Miller, S. K. R.; Banks, B. *MRS Bull.* **2010**, *35*, 20.
(7) Rutledge, S. K.; Mihelcic, J. A. The Effect of Atomic Oxygen on Altered and Coated Kapton Surfaces for Spacecraft Applications in Low Earth Orbit. In *Proceedings of a Symposium Sponsored by TMS-ASM Joint Corrosion and Environmental Effects Committee and the 199th Annual Meeting of the Minerals, Metals, and Materials Society*; Anaheim, CA, 1990; The Minerals, Metals, and Materials Society: Warrendale, PA, 1990.
(8) Rutledge, S. K.; Olle, R. M. Space Station Freedom Solar Array Blanket Coverlay Atomic Oxygen Durability Testing Results. In *Proceedings of the 38th International SAMPE Symposium*; Anaheim, CA, 2003; Society for the Advancement of Material and Process Engineering: Covina, CA, 1993.
(9) Brunsvold, A. L.; Minton, T. K.; Gouzman, I.; Grossman, E.; Gonzalez, R. *High Perform. Polym.* **2004**, *16*, 303.
(10) Tennyson, R. C. *High Perform. Polym.* **1999**, *11*, 157.
(11) George, S. M. *Chem. Rev.* **2010**, *110*, 111.
(12) George, S. M.; Ott, A. W.; Klaus, J. W. *J. Phys. Chem.* **1996**, *100*, 13121.
(13) Dillon, A. C.; Ott, A. W.; Way, J. D.; George, S. M. *Surf. Sci.* **1995**, *320*, 230.
(14) Ferguson, J. D.; Weimer, A. W.; George, S. M. *Chem. Mater.* **2004**, *16*, 5602.
(15) Wilson, C. A.; Grubbs, R. K.; George, S. M. *Chem. Mater.* **2005**, *17*, 5625.
(16) Groner, M. D.; Elam, J. W.; Fabreguette, F. H.; George, S. M. *Thin Solid Films* **2002**, *413*, 186.
(17) Carcia, P. F.; McLean, R. S.; Reilly, M. H.; Groner, M. D.; George, S. M. *Appl. Phys. Lett.* **2006**, *89*, 031915.
(18) Groner, M. D.; George, S. M.; McLean, R. S.; Carcia, P. F. *Appl. Phys. Lett.* **2006**, *88*, 051907.
(19) Cooper, R.; Upadhyaya, H. P.; Minton, T. K.; Berman, M. R.; Du, X.; George, S. M. *Thin Solid Films* **2008**, *516*, 4036.
(20) Ritala, M.; Leskela, M.; Nykanen, E.; Soininen, P.; Niinisto, L. *Thin Solid Films* **1993**, *225*, 288.
(21) Aarik, J.; Aidla, A.; Uustare, T.; Sammelselg, V. *J. Cryst. Growth* **1995**, *148*, 268.
(22) Cameron, M. A.; Gartland, I. P.; Smith, J. A.; Diaz, S. F.; George, S. M. *Langmuir* **2000**, *16*, 7435.
(23) Zhang, J.; Garton, D. J.; Minton, T. K. *J. Chem. Phys.* **2002**, *117*, 6239.
(24) Zhang, J.; Upadhyaya, H. P.; Brunsvold, A. L.; Minton, T. K. *J. Phys. Chem. B* **2006**, *110*, 12500.
(25) Buczala, D. M.; Brunsvold, A. L.; Minton, T. K. *J. Spacecr. Rockets* **2006**, *43*, 421.
(26) Elam, J. W.; Groner, M. D.; George, S. M. *Rev. Sci. Instrum.* **2002**, *73*, 2981.
(27) Ranby, B.; Babek, J. F. *Photodegradation, Photooxidation, and Photostabilization of Polymers, Principles and Applications*; Wiley: London, 1975.
(28) Okudaira, K. K.; Hasegawa, S.; Sprunger, P. T.; Morikawa, E.; Saile, V. S., K.; Harada, Y.; Ueno, N. *J. Appl. Phys.* **1998**, *83*, 4292.
(29) Cisse, A. L. Photodegradation of PMMA and Application in Surface and Diffusion Studies. *Ph.D. Thesis*, The University of Chicago, Chicago, 2007.
(30) Zhang, J.; Lindholm, N. F.; Brunsvold, A. L.; Upadhyaya, H. P.; Minton, T. K.; Tagawa, M. *ACS Appl. Mater. Interfaces* **2009**, *1*, 653.
(31) Jellison, G. E.; Boatner, L. A.; Budai, J. D.; Jeong, B. S.; Norton, D. P. *J. Appl. Phys.* **2003**, *93*, 9537.

AM100217M